International Journal of Engineering and Applied Sciences (IJEAS)
ISSN: 2394-3661, Volume-3, Issue-8, August 2016

~~Comparing between Hysteresis Current Controller and Space Vector Modulation of Field Oriented Control when Driving PMSM~~

Hamdy Mohamed Soliman

***Abstract*— There are many methods to drive the AC motors. The motor which used here is permanent magnet synchronous motor. From the best method to drive these motors is field oriented control. The field oriented control can be used with hysteresis current control and with the space vector modulation. So this paper is compared between the hysteresis current controller and with space vector modulation. This comparison depends upon what is the hysteresis current controller and what is the space vector modulation, how to build each method, torque ripples for each method and total harmonic distortion in the current and in the voltage for each method. MALTAB is used to simulate these methods.**

***Index Terms*—Hysteresis current control, Field oriented control, Permanent magnet synchronous motor and Space vector modulation.**

I. INTRODUCTION

With discover the rare earth materials, the scientist and researchers realize the supper magnetic properties of these materials. So they make many alloys from these materials to get supper permanent magnets but these alloys have disadvantages as high cost and effected by high temperature. With development of industrial technology for these materials, the disadvantages are solved i.e. the cost of these materials are reduced and become less sensitive for high temperature so it is used in the electrical machines to improve the performance characteristics. From these machines which used the permanent magnet materials, the synchronous machines where the rotor windings are replaced by permanent magnet materials. This added some advantages for synchronous machine such as long operating life, high torque to current ratio, quick acceleration and deceleration, rotor becomes lossless, no brushes are used and high efficiency. For these reasons, this paper uses the permanent magnet synchronous motor (PMSM) in this study. Here the principle operation of the field oriented control (FOC) with hysteresis current control (HCC) and with space vector modulation (SVM) are compared to show the advantages and disadvantages of each method [1-4]. This can be done by how to build each one, the results of simulation for both of them, deduced from simulation the different in transient response between them, and in the steady state the amount of torque ripples, total harmonic distortion in the current and in the voltage. This paper is classified into I- introduction II- mathematical model of PMSM III-field oriented control of PMSM VI- hysteresis current controller of PMSM V- space vector modulation of PMSM VI-simulation results VII-conclusions.

Dr. Hamdy Mohamed Soliman, B. Sc. in Electrical Power and Machine Engineering, master of science in area of electrical machine and drive systems., PhD Degree from Cairo University, Giza, Egypt

II. MATHEMATICAL MODEL OF PMSM

The mathematical model of a PMSM is similar to that of wound rotor synchronous motor. The rotor winding of synchronous motor is replaced with high resistivity permanent magnet material, hence, induced current in the rotor are negligible. The rotor types of PMSM are shown in Fig.1. The permanent magnets on the rotor are shaped in such a way as to produce sinusoidal back EMF in stator windings.

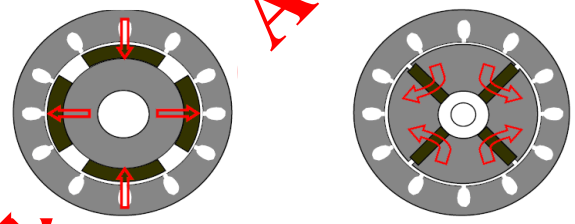

(a) PM surface mounted (b) PM surface interior (buried)

Fig 1. The types of the rotor in PMSM

The following equations represent the mathematical model of the PMSM

$$v_d = r_s i_d + L_d \frac{d(i_d)}{dt} - \omega_r L_q i_q \quad (1)$$

$$v_q = r_s i_q + L_q \frac{d(i_q)}{dt} + \omega_r L_d i_d + \omega_r \psi_m \quad (2)$$

$$T_e = \frac{3}{4} P(\psi_m + (L_d - L_q) i_d) i_q \quad (3)$$

$$T_e = T_L + \beta \omega_r + J \frac{2}{P} \frac{d\omega_r}{dt} \quad (4)$$

$$\theta_r = \frac{P}{2} \int \omega_m \, dt \quad (5)$$

Where v_d, v_q are the dq axes stator voltages, i_d, i_q are the dq axes stator currents, L_d, L_q are the dq stator axis inductance, r_s is a stator resistance, $\frac{d}{dt}$ is a derivative, T_e is an electrical torque, T_L is a load torque, J is a moment of inertia, β is a frictional viscous, ω_m is a mechanical speed, P is a number of poles and θ_r is an electrical position.

III. FIELD ORIENTED CONTROL OF PMSM

The field oriented control makes the PMSM emulates the separately excited DC motor. To understand this let's start with the principle torque equation

$$T_e \alpha \psi_s \psi_r \sin\varepsilon \cos\Gamma \quad (6)$$

Where ψ_s and ψ_r are stator and rotor flux linkages, ε and Γ are the space and time angles between stator and rotor flux linkages. If it is applied on DC machine it is found that,

The space angle is equal to 90° and time angle is 0° because the field comes from DC field hence the torque equation becomes as the follows

$$T_e \alpha \psi_s \psi_r \quad (7)$$

This means that, the torque becomes maximum value. By applying this equation on permanent magnets synchronous motor it is found that, the space angle is smaller than 90° and hence, to verify the same torque taken from DC, it must be increased the stator flux, by such an increase the stator current and hence it is found that, the torque per ampere of DC is higher than the torque per ampere of PMSM [5-6]. By applying the FOC or vector control it is found that, the torque problem is solved and this will be discussed later. Fig. 2 shows the DC and PMSM space angle where it is found that,

DC motor has constant space angle 90° where PMSM has varying one which increases by increasing the load, it reaches 90° at maximum load.

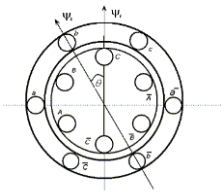

(a) Space angle between rotor and stator fluxes of permanent magnet synchronous motor

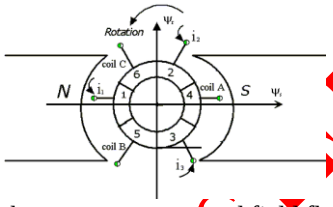

(b) Space angle between armature and field flux of DC motor
Fig. 2 Space angle for DC motor and permanent magnet synchronous motor between rotor and stator fluxes.

When comparing between the armature current for both of DC motor and PMSM, it is found that, the armature current of DC motor increases from zero linearly by increasing the load where in PMSM, the current becomes higher at low loads and increased by higher values by increasing the load as shown in the Fig. 3. This means that, the torque per ampere of DC motor is higher than the torque per ampere in permanent magnet synchronous motor hence there are many models to improve the torque per ampere in PMSM by making the space angle between rotor and stator field always 90° at any load and speed of the motor. This control is called FOC. With FOC, the stator current is analyzing into two independently components one of the field (i_d) corresponding to the DC field current and the other (i_q) corresponding to the DC armature current. The FOC control system generates the required magnitude and phase voltage at certain frequency to impress the exact stator current that will give the desired torque. The speed controller calculates a reference torque, which is proportional to the quadrature-axis stator current component i_q^*. The direct-axis stator current component i_d^* is set to zero if there is no field weakening. This occurs only in the constant flux region so with FOC the torque becomes

$$T_e = \frac{3}{4} P(\psi_m I_q) \quad (8)$$

But in the field weakening region $i_d \neq 0$. In this region, the motor rotates beyond the base speed. Here the field flux is inversely proportional to speed. The principle operation of FOC in this region is an increase the negative direct axis current component and uses the armature reaction to reduce the air gap flux. The stator voltages tend to saturate so the stator flux must be weakened beyond the base speed. In this method the torque is changed by variation the angle between MMF of the stator and the rotor d-axis. This means that a demagnetizing current $(-i_d)$ must be injected so the (i_q) is calculated from the following relation

$$i_q = \sqrt{I_m^2 - (-i_d)^2} \quad (9)$$

The model of permanent magnet synchronous motor in field coordinates can be represented by the block diagram of Fig. 4.

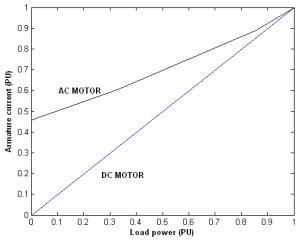

Fig. 3 Variation of armature current with load power in case of permanent magnet synchronous motor and DC motor.

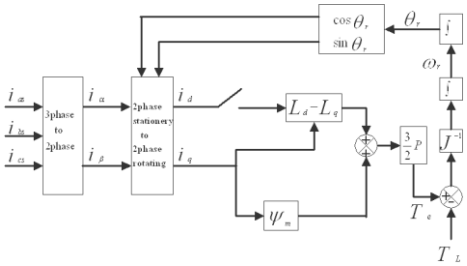

Fig. 4 Block diagram of permanent magnet synchronous motor in field coordinates.

IV. Hysteresis Current Control of PMSM

The block diagram of the PMSM drive system with using HCC is given Fig. 5, the drive system is composed of two blocks, the first is for FOC and the other is to regulate the current. Fig. 6 shows the details of the first block (FOC block). It contains only one PI controller (speed controller) to deduce the reference torque current component. In the current regulator block, the hysteresis current controller is used due to simple, fast dynamic response and insensitive to load parameters. The hysteresis current controller is shown in Fig. 7. In this method each phase consists of comparator and hysteresis band. The switching signals are generated due to error in the current. The error comes from comparing between the reference current and actual current. The main task of this method of control is to make the input current to close the reference current in each phase. The deviation of these currents (error current) represents the current distortion. The THD in the current can be calculated as

The current distortion $= \frac{100}{I_{rms}} \sqrt{\frac{1}{T}\int (i_{act} - i_{ref})^2 dt}$ % (10)

In this method of control, the deviation of the current is between two limits of the hysteresis band (upper and lower).

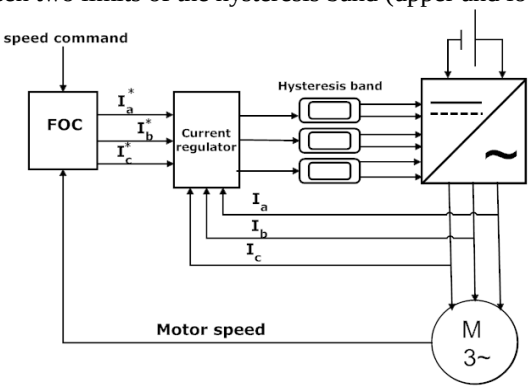

Fig. 5 Block diagram of PMSM drive system

In any phase, if the actual current becomes more than the upper limit of hysteresis band, the higher switch of the inverter arm becomes off and complementary switch on and the current starts to decay. In contrast if the actual current reaches lower limit of the band, the lower switch of the inverter arm is off, the upper switch is on and the current comes back into the hysteresis band. The band width of hysteresis calculates the switching frequency and current ripple.

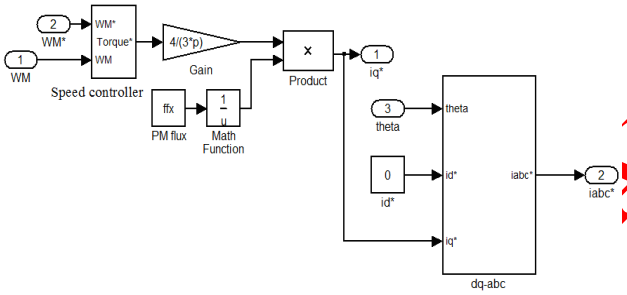

Fig. 6 FOC details for classical and modified methods

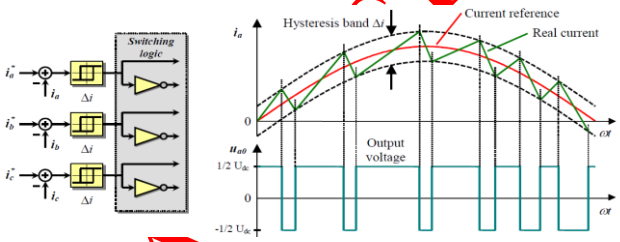

Fig. 7 Hysteresis PWM current control and switching logic

V. SPACE VECTOR MODULATION OF PMSM

SVM technique is used to switching the three phase inverter in drive system. This can be seen in Fig.8. It is consisting of six switches that shape the output voltages. When any upper switch is on, the lower switch in the same arm is off so by known the upper switched case and the output voltage can be determined [7-9]. The relation between the line to line voltages and switching state can be calculated from the following relation

$$\begin{pmatrix} v_{ab} \\ v_{bc} \\ v_{ca} \end{pmatrix} = v_{dc} \begin{pmatrix} 1 & -1 & 0 \\ 0 & 1 & -1 \\ -1 & 0 & 1 \end{pmatrix} \begin{pmatrix} a \\ b \\ c \end{pmatrix} \quad (11)$$

The relation between the phase voltages and switching state can be calculated from the following relation

$$\begin{pmatrix} v_{an} \\ v_{bn} \\ v_{cn} \end{pmatrix} = \frac{v_{dc}}{3} \begin{pmatrix} 2 & -1 & -1 \\ -1 & 2 & -1 \\ -1 & -1 & 2 \end{pmatrix} \begin{pmatrix} a \\ b \\ c \end{pmatrix} \quad (12)$$

From Fig.8 it is found that, eight possible connections state (on off patterns) these pattern states (V_0, V_1, V_2, V_3, V_4, V_5, V_6, V_7) are given in table1. From this table, the eight switching vector can be represented as Fig.9. Each of these space vectors in Fig.10 resulted from two adjacent vectors and any zero vectors (V_0, V_7).

Space vector pulse width modulation (SVPWM) can be implemented in the following steps:

- Calculate v_α, v_β, v_{ref} and angle α
- Calculate the time duration T_1, T_2 and T_s
- Calculate the switching time of each switches (T1 to T6)

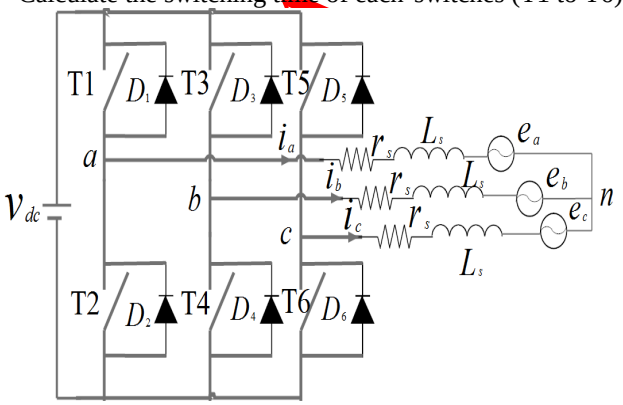

Fig.8. Power circuit inverter and PMSM

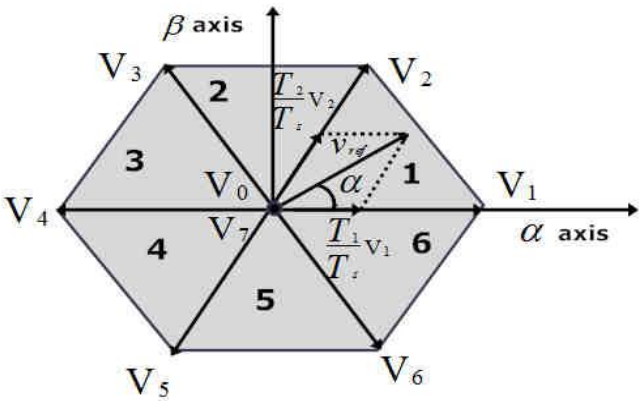

Fig.9. Switching space vector and sector

A. Calculate v_α, v_β, v_{ref} and Angle α

Depending upon Fig. 10; the v_{ref} and angle α can be calculated as

$$v_{ref} = \sqrt{v_\alpha^2 + v_\beta^2} \quad (13)$$

$$\alpha = \arctan\left(\frac{v_\beta}{v_\alpha}\right) \quad (14)$$

B. Calculate the time duration T_1, T_2 and T_s

Depending upon Fig.10 to calculate the time duration in sector1 on the real and imaginary axes it is found that;

$$\frac{T_1}{T_s}v_1+\frac{T_1}{T_s}v_2\cos 60^0 = mv_{ref}\cos\alpha \quad (15)$$

$$\frac{T_2}{T_s}v_2\sin 60^0 = mv_{ref}\sin\alpha \quad (16)$$

From (15) and (16) it is found that;

$$T_1=\frac{\sqrt{3}}{2}mT_s\sin(60-\alpha) \quad (17)$$

$$T_2=\frac{\sqrt{3}}{2}mT_s\sin\alpha \quad (18)$$

$$T_0=T_s-(T_1+T_2) \quad (19)$$

Where $T_s=\frac{1}{F_s}$ is switching frequency and *m* is modulation index

From that the switching time duration at any sector can be calculated as:

$$T_1=\frac{\sqrt{3}}{2}mT_s\sin(n\frac{\Pi}{3}-\alpha) \quad (20)$$

$$T_2=\frac{\sqrt{3}}{2}mT_s\sin((n-1)\frac{\Pi}{3}-\alpha) \quad (21)$$

Where *n* is the number of sector

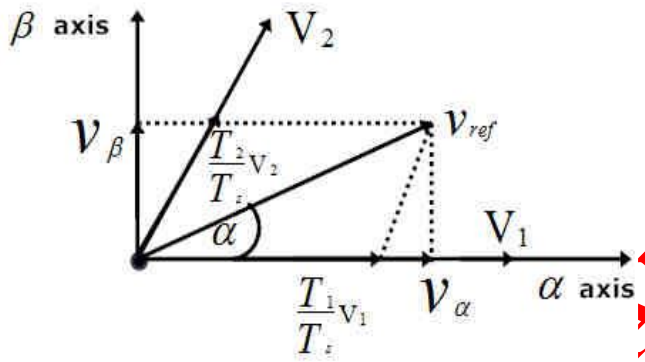

Fig. 10 Voltage sector v_{ref}

Voltage vector	Switching on	Line to neutral voltage			Line to line voltage		
		v_{an}	v_{bn}	v_{cn}	v_{ab}	v_{bc}	v_{ca}
V0	T1,T3,T5	0	0	0	0	0	0
V1	T2,T3,T5	2/3	-1/3	-1/3	1	0	-1
V2	T2,T4,T5	1/3	1/3	-2/3	0	1	-1
V3	T1,T4,T5	-1/3	2/3	-1/3	-1	1	0
V4	T1,T4,T6	-2/3	1/3	1/3	-1	0	1
V5	T1,T3,T6	-1/3	-1/3	2/3	0	-1	1
V6	T2,T3,T6	1/3	-2/3	1/3	1	-1	0
V7	T2,T4,T6	0	0	0	0	0	0

Table 1. Modes of operation of the three phase voltage source inverter in term of v_{dc}

C. *Calculate the switching time of each switches (T1 to T6)*

Table2 shows the switching time in inverter.

The SVM structure of the field oriented control is shown in Fig.11. The error in q axis current is introduced to PI current controller to produce q axis voltage reference also the error in d axis current is delivered to PI current controller to produce d-axis voltage reference. These voltages are transformed with help of electrical rotor position into two dimensional voltages varying in time which used to generate gating signals to drive the inverter through SVM

sector	Upper switches	Lower switches

	(T1,T3,T5)	(T2,T4,T6)
1	T1= $T_1+T_2+\frac{T_0}{2}$ T3= $T_2+\frac{T_0}{2}$ T5= $\frac{T_0}{2}$	T2= $\frac{T_0}{2}$ T4= $T_2+\frac{T_0}{2}$ T6= $T_1+T_2+\frac{T_0}{2}$
2	T1= $T_2+\frac{T_0}{2}$ T3= $T_1+T_2+\frac{T_0}{2}$ T5= $\frac{T_0}{2}$	T2= $T_2+\frac{T_0}{2}$ T4= $\frac{T_0}{2}$ T6= $T_1+T_2+\frac{T_0}{2}$
3	T1= $T_1+T_2+\frac{T_0}{2}$ T3= $T_2+\frac{T_0}{2}$ T5= $\frac{T_0}{2}$	T2= $T_1+T_2+\frac{T_0}{2}$ T4= $\frac{T_0}{2}$ T6= $T_2+\frac{T_0}{2}$
4	T1= $\frac{T_0}{2}$ T3= $T_2+\frac{T_0}{2}$ T5= $T_1+T_2+\frac{T_0}{2}$	T2= $T_1+T_2+\frac{T_0}{2}$ T4= $T_2+\frac{T_0}{2}$ T6= $\frac{T_0}{2}$
5	T1= $T_2+\frac{T_0}{2}$ T3= $\frac{T_0}{2}$ T5= $T_1+T_2+\frac{T_0}{2}$	T2= $T_2+\frac{T_0}{2}$ T4= $T_1+T_2+\frac{T_0}{2}$ T6= $\frac{T_0}{2}$
6	T1= $T_1+T_2+\frac{T_0}{2}$ T3= $\frac{T_0}{2}$ T5= $T_2+\frac{T_0}{2}$	T2= $\frac{T_0}{2}$ T4= $T_1+T_2+\frac{T_0}{2}$ T6= $T_2+\frac{T_0}{2}$

Table 2. Switching time duration

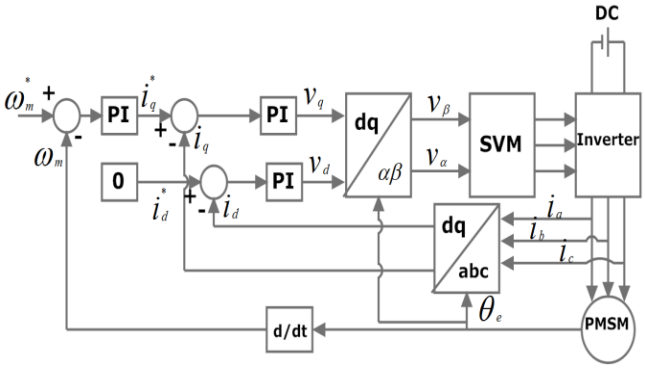

Fig.11. Space vector modulation structure field oriented control

VI. Simulation Results

Here hysteresis current controller and SVM with FOC are compared. These comparisons are simulated by MATLAB program. Table3 shows the difference between the hysteresis current controller and SVM in term of torque ripples and total harmonics distortion in current and voltage. Appendix (1) shows the motor parameters which used in this simulation. During the simulations, the torque set value is at rated. In all

Figs the time axis is in seconds and the following cases are simulated

1. Motor starting with full loading.
2. Sudden applied and removal the rated load.
3. Reversing speed at rated load

Where it is found that,

A. The First Case (starting with rated load)

Figs (12-13) show the variation of the stator flux with HCC and with SVM respectively. From these Figs. can be concluded that; the distortion in the stator flux is less with SVM.

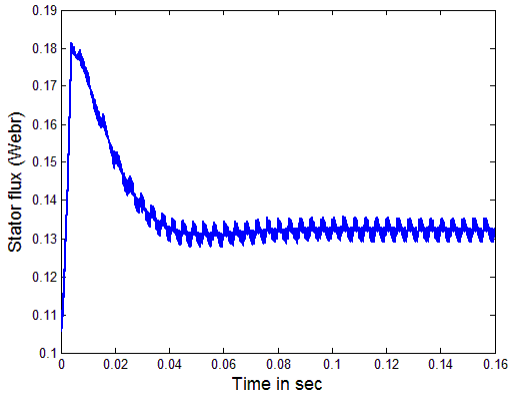

Fig. 12 Stator flux with hysteresis current control

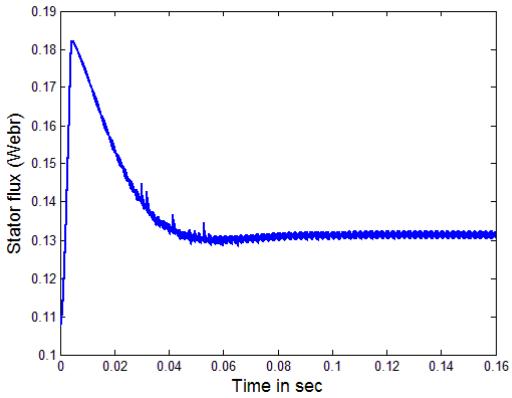

Fig. 13 Stator flux with space vector modulation

Figs (14-15) show the variation of torque current component and flux current component with HCC and with SVM respectively. From these Figs. can be concluded that; the d-axis stator current has value at starting with the SVM and return to zero after that. The d and q current components is less ripples with the SVM.

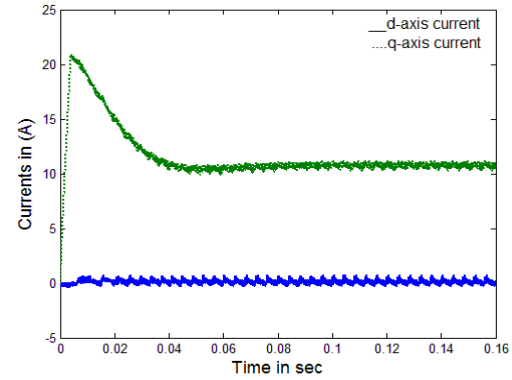

Fig. 14 dq axes current with hysteresis current control

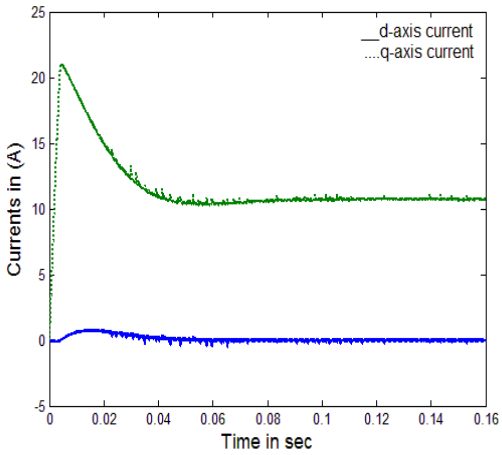

Fig. 15 dq axes current with space vector modulation

Figs (16-17) show the variation of motor torque compared load torque with HCC and with SVM respectively. From these Figs. can be concluded that; with HCC the motor torque reached the steady state load torque faster than the SVM method. The SVM method is less ripples torque in it is compared to HCC method.

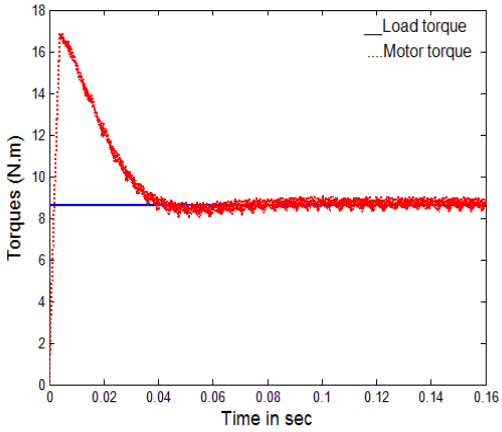

Fig. 16 Torque with hysteresis current control

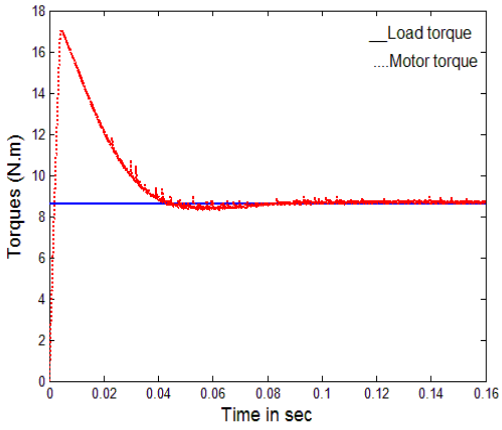

Fig. 17 Torque with space vector modulation

Figs (18-19) show the variation of the motor speed with HCC and with SVM respectively. From these Figs. can be concluded that; with HCC the motor speed reached the steady state speed faster than the SVM method.

Figs (20-21) show the variation of the stator current with HCC and with SVM respectively. From these Figs. can be concluded that; The SVM method is less in the total harmonic distortion if it is compared to HCC method.

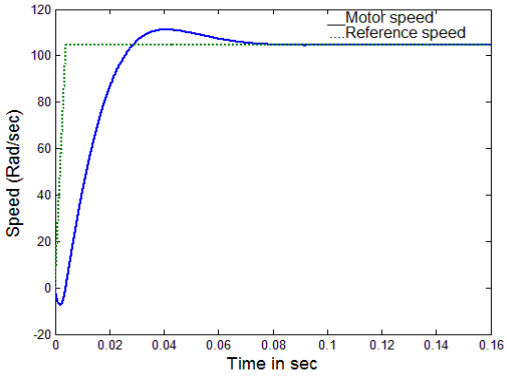

Fig. 18 Speed with hysteresis current control

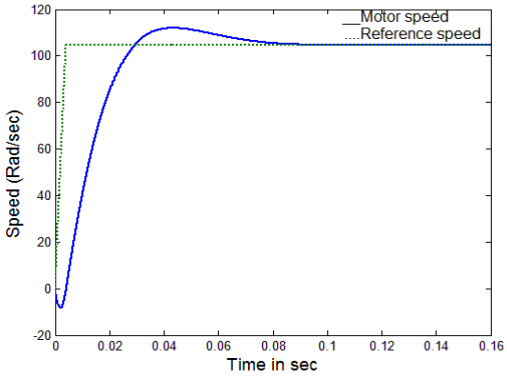

Fig. 19 Speed with space vector modulation

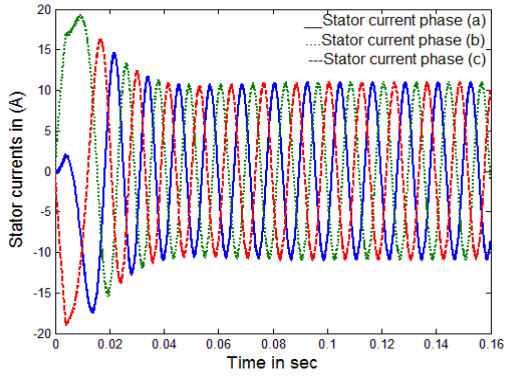

Fig. 20 Stator current with hysteresis current control

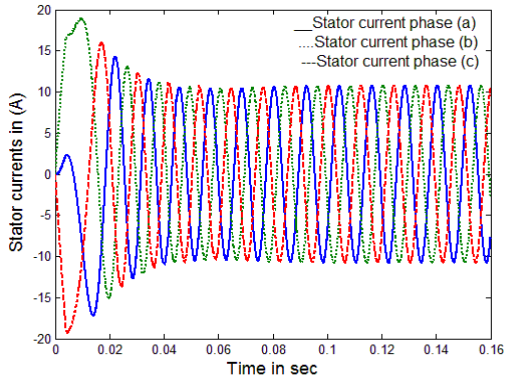

Fig. 21 Stator current with space vector modulation

B. The Second Case (sudden applied and removal the rated load)

Figs (22-23) show the variation of torque current component and flux current component with HCC and with SVM respectively. From these Figs. can be concluded that; The d and q current components is less ripples with the SVM.

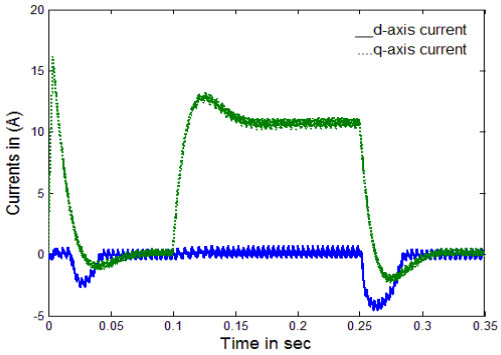

Fig. 22 dq axes current with hysteresis current control

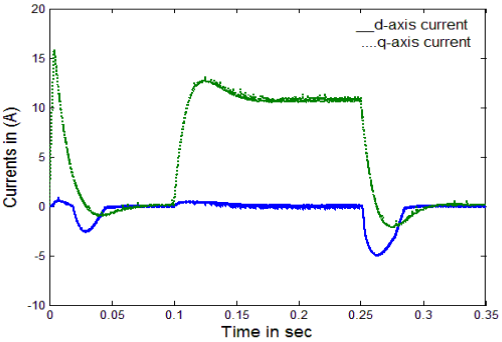

Fig. 23 dq axes current with space vector modulation

Figs (24-25) show the variation of motor torque compared load torque with HCC and with SVM respectively. From these Figs. can be concluded that; with HCC the motor torque reached the steady state load torque faster than the SVM method. The SVM method is less ripples torque in it is compared to HCC method.

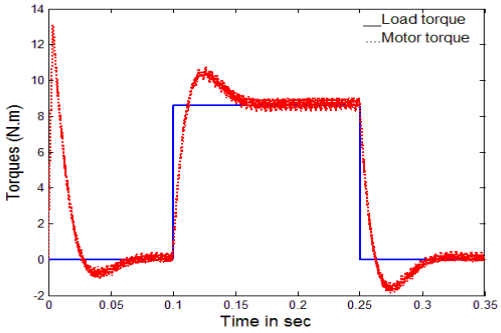

Fig. 24 Torque with hysteresis current control

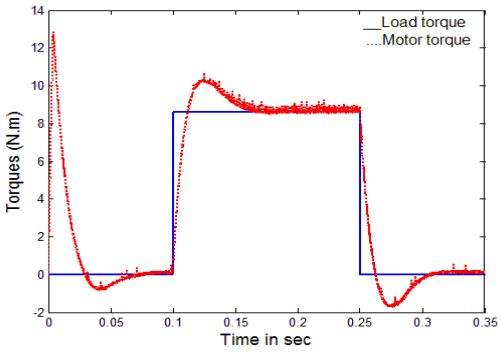

Fig. 25 Torque with space vector modulation

Figs (26-27) show the variation of the motor speed with HCC and with SVM respectively. From these Figs. can be concluded that; with HCC the motor speed reached the steady state speed faster than the SVM method.

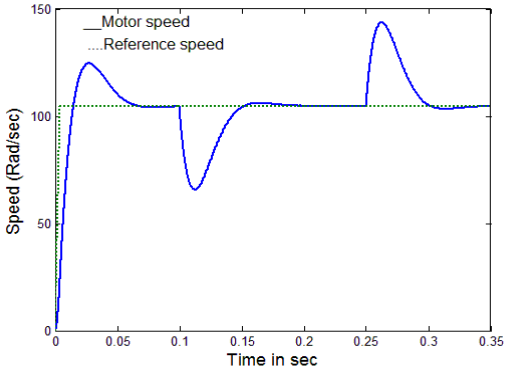

Fig. 26 Speed with hysteresis current control

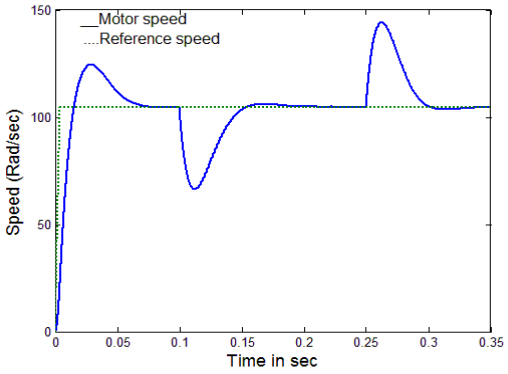

Fig. 27 Speed with space vector modulation

Figs (28-29) show the variation of the stator current with HCC and with SVM respectively. From these Figs. can be concluded that; The SVM method is less in the total harmonic distortion if it is compared to HCC method.

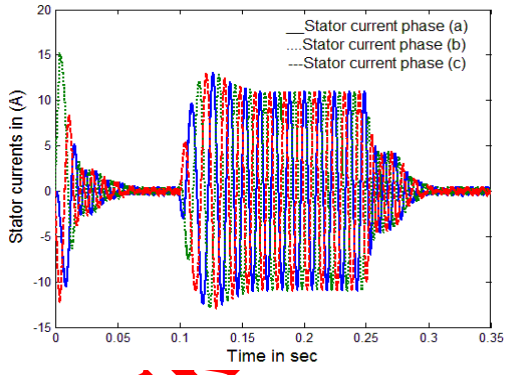

Fig. 28 Stator current with hysteresis current control

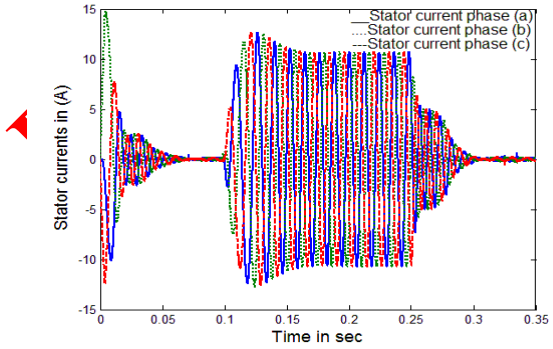

Fig. 29 Stator current with SVM

C. The Third Case (reversing speed with rated load)

Figs (30-31) shows the variation of the dq-axes currents with HCC and with SVM respectively. From these Figs. can be concluded that; the SVM is more effecting by reversing speed.

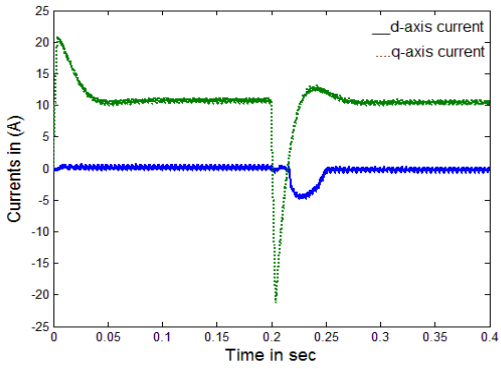

Fig. 30 dq axes current with hysteresis current control

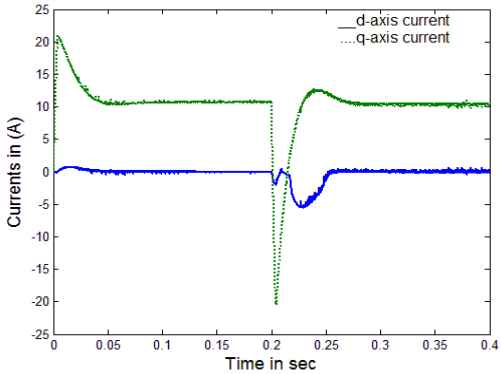

Fig. 31 dq axes current with space vector modulation

Figs (32-33) the variation of motor torque compared load torque with HCC and with SVM respectively. From these Figs. can be concluded that; with HCC the motor torque reached the steady state load torque faster than the SVM method. The SVM method is less ripples torque in it is compared to HCC method. Also in these methods the motor torque is reversing when motor speed reversing.

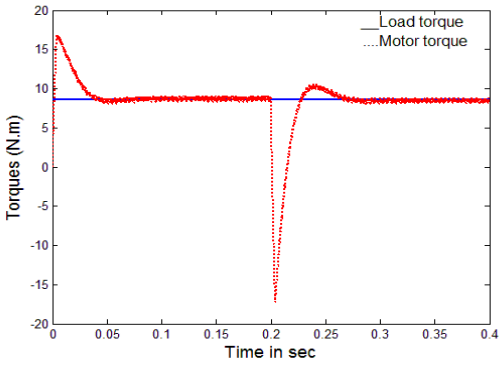

Fig. 32 Torque with hysteresis current control

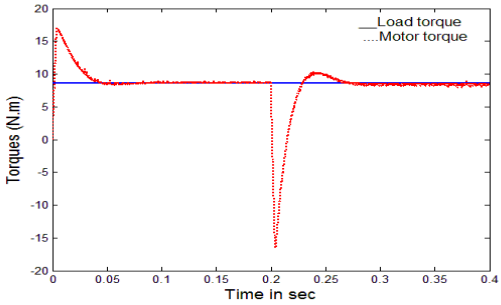

Fig. 33 Torque with space vector modulation

Figs (34-35) shows the variation of the motor speed with HCC and with SVM respectively. From these Figs. can be

concluded that; with HCC the motor speed reached the steady state speed faster than the SVM method.

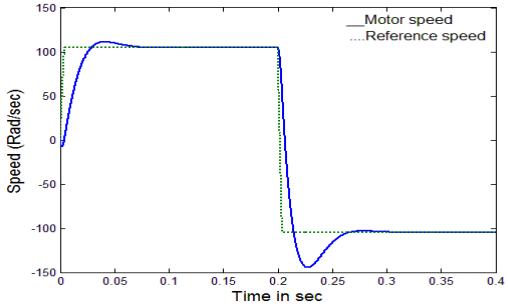

Fig. 34 Speed with hysteresis current control

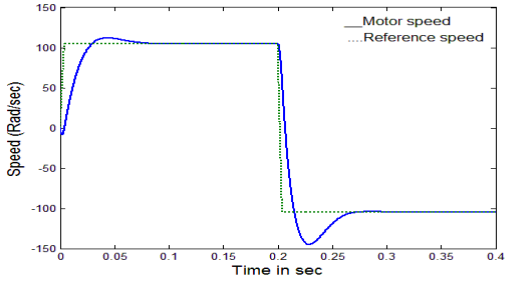

Fig. 35 Speed with space vector modulation

Figs (36-37) show the variation of the stator current with HCC and with SVM respectively. From these Figs. can be concluded that; The SVM method is less in the total harmonic distortion if it is compared to HCC method. Also the current is reversing at reversing speed.

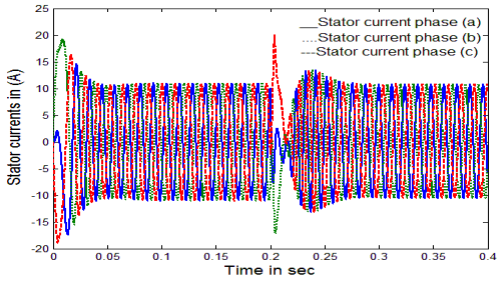

Fig. 36 Stator current with hysteresis current control

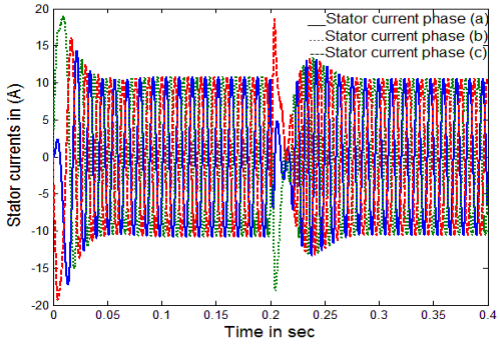

Fig. 37 Stator current with space vector modulation

VII. Conclusion

HCC and the SVM with FOC are explained and are simulated through the MATLB program. The simulation shows that; the HCC with FOC is faster if it is compared to SVM with FOC. The torque ripples are less with SVM compared to HCC. The total harmonics in current are less with SVM compared to hysteresis current controller. The total harmonics in voltage are less with SVM compared to hysteresis current controller.

Method of control	THD in volt	THD in current	Torque ripples
HCC with FOC	90.1	2.38	1.56
SVM with FOC	84.13	0.72	0.57

Table 3 Effect of modified methods on the THD in voltage, current and torque ripples

Appendix (1)

Motor data

Line to line voltages	110V
Inertia	0.001118Kg.m^2
Magnetic flux linkage	0.108Wb
Pole pairs	5
Rated power	900W
Rated speed	1000 R.P.M
Stator resistance	0.436ohm
q-axis inductance	6.97mH
d-axis inductance	6.97mH

References

[1] Goed, I. da Silva and P. Jose, A. Serni, "A hybrid controller for the speed control of a permanent magnet synchronous motor drive," *Control Engineering Practice*, Vol. 16, Issue 3, pp. 260-270, March, 2008.

[2] C. Mademlis and N. Margaris, "Loss minimization in vector-controlled interior permanent-magnet synchronous motor drives", *Industrial Electronics, IEEE Transactions on*, vol. 49, pp. 1344-1347, 2002.

[3] X. Jian-Xin, S. K. Panda, P. Ya-Jun, L. Tong Heng, and B. H. Lam, "A modular control scheme for PMSM speed control with pulsating torque minimization", *Industrial Electronics, IEEE Transactions on*, vol. 51, pp. 526-536, 2004.

[4] Hamdy Mohamed soliman and S. M. EL. Hakim," Improved Hysteresis Current Controller to Drive Permanent Magnet Synchronous Motors Through the Field Oriented Control", *International Journal of Soft Computing and Engineering*, Vol. 2, No. 4, pp. 40-46, September 2012.

[5] D. M. Brod and D. W. Novotny, "Current Control of VSI-PWM Inverters," *IEEE Trans. on Industry App.* vol. IA-21. no. 4, May/June 1985.

[6] Phoivos D.Ziogas, "The Delta Modulation Technique in Static PWM Inverters" *IEEE Transactions on Industrial Applications*,pp.199-204, March/April 1981.

[7] A. Lidozzi, L. Solero, F. Crescimbini, and A. Di Napoli, "SVM PMSM drive with low resolution Hall-effect sensors," *IEEE Trans Power Electron.*, vol. 22, no. 1, pp. 282–290, Jan. 2007.

[8] D. Swierczynski and M. P. Kazmierkowski, Direct Torque Control of Permanent Magnet Synchronous Motor (PMSM) Using Space Vector Modulation (DTC-SVM) – simulation and experimental results, *in Conf. Proc. IEEE 28th Annual Conference of the Industrial Electronics Society (IECON'02)*, vol. 1, Nov. 5–8, 2002, pp. 751–755.

[9] *E* Jenni and F. Wueest, "The optimization parameters of space vector modulation," *in Proc. 5th European Conf. Power Electronics and Applications*, pp.376-381, 1993.

Dr. Hamdy Mohamed Soliman was born in Cairo-Egypt on 26 December 1970, He received B. Sc. in Electrical Power and Machine Engineering from Helwan University in 1993, master of science in area of electrical machine and drive systems. Master of science is from Benha University and PhD Degree from Cairo University, Giza, Egypt in 2016. The area of PhD is electrical machines and drives. He is a director of development and research of train units in Egyptian company metro. His current research interests include power electronics, motor controls and drive systems